

# Simultaneously Improved Toughness and Dielectric Properties of Epoxy/Core-Shell Particle Blends

Weitao Wan,<sup>1,2</sup> Demei Yu,<sup>1,2</sup> Jian He,<sup>1</sup> Yunchuan Xie,<sup>1,2</sup> Longbiao Huang,<sup>1</sup> Xiusheng Guo<sup>1,2</sup>

<sup>1</sup>Department of Applied Chemistry, Xi'an Jiaotong University, Xi'an 710049, People's Republic of China

<sup>2</sup>State Key Laboratory of Electrical Insulation and Power Equipment, Xi'an Jiaotong University, Xi'an 710049, People's Republic of China

Received 11 November 2006; accepted 1 January 2007

DOI 10.1002/app.26102

Published online 1 October 2007 in Wiley InterScience (www.interscience.wiley.com).

**ABSTRACT:** Epoxy/core-shell particle blends were prepared using a diglycidylether of bisphenol A epoxy and acrylics-type core-shell particles. The impact strength of the blends was tested, and the result showed that the epoxy was greatly toughened with optimum core-shell particle content. Meanwhile, the dielectric properties of both epoxy and its blends were investigated using a broadband dielectric analyzer. It was found that the dielectric constant of the epoxy blends with lower core-shell particle content were less than that of the epoxy in the investigated frequency range, while the dielectric loss was less than that of the neat epoxy over a low frequency range, even for the epoxy blends with the optimum core-shell particle content. The dielectric breakdown strength

of the epoxy blends at room and cryogenic temperature were also investigated. To identify the primary relationship of the above properties and structure of the epoxy blends, the microstructure of the core-shell particle and the morphology of the samples were observed by transmission electron microscopy and scanning electron microscopy. It was considered that these epoxy/core-shell particle blends with improved toughness and desirable dielectric properties could have a potential application in the insulation of electronic packaging system. © 2007 Wiley Periodicals, Inc. *J Appl Polym Sci* 107: 1020–1028, 2008

**Key words:** dielectric properties; toughness; epoxy; core-shell particles; electric modulus

## INTRODUCTION

Epoxy resins have been widely used in aerospace, semiconductor, and microelectronic industry, especially for electrical insulation system because of their excellent chemical and dimensional stability, as well as good adhesive and dielectric properties. However, the well-known drawbacks of epoxy resin are their inherent brittleness, which limit a further application of epoxy resin under severe conditions. For this reason, ways to improve the toughness of epoxy resin have been studied intensively in recent years. Besides modifying epoxy resin with liquid rubbers,<sup>1–5</sup> it's usually considered that modifying epoxy resin with core-shell particles is a good way to solve the toughness problem. It may be because of the unique multilayer structure of core-shell particles.<sup>6–10</sup>

As we know, if epoxy resins are used as insulating materials for electronic packaging applications or inte-

grated circuit fields, it is necessary to meet the requirements of good toughness and dielectric properties, such as low dielectric constant, low dielectric loss, and high dielectric breakdown strength. When epoxy resins are toughened by core-shell particles, some dipolar groups (—OH, —COOH, etc.) would be introduced. Simultaneously some interfaces would also be introduced and interfacial polarizations could occur in the bulk epoxy under applied electrical field.<sup>11</sup> The implanted dipolar groups and the interfacial polarizations will affect the overall dielectric properties of the epoxy resins. However, there have been few reports on the epoxy/core-shell particle blends with improved dielectric properties and toughness simultaneously. In this article, the epoxy was modified by core-shell particles. The dielectric behavior of the toughened epoxy blends over a broad frequency range was investigated at room temperature, as well as the dielectric breakdown strength at room and cryogenic temperature. The impact property of the modified epoxy was also tested.

## EXPERIMENTAL

### Materials

The epoxy used in this study was a diglycidylether of bisphenol A (DGEBA; 6101, Wuxi Resin Factory of

Correspondence to: D. Yu (dmyu@mail.xjtu.edu.cn).

Contract grant sponsor: National Natural Science Foundation; contract grant number: 50177026.

Contract grant sponsor: State Key Laboratory of Electrical Insulation and Power Equipment, People's Republic of China.

Blue New Chemical Materials, Jiangsu province, China) with an equivalent weight of 250 g/equiv. and average molecular weight  $M_n = 450$ . The curing agent was methyltetrahydrophthalic anhydride, MTHPA (Xi'an Resin Factory, Shaanxi province, China). The accelerator was 2,4,6-tri (dimethylaminomethyl) phenol (DMP30, Shanghai Chemical Reagent Factory, Shanghai, China). The core-shell particles (EXL-2330) were commercially available from Rohm and Haas, which consisted of crosslinked poly (butylacrylate) core and grafted poly (methylmethacrylate) shell. The chemical structures of the reagents and core-shell particles were described in Table I.

### Sample preparation

The epoxy/core-shell particle blends were prepared as follows. After heating the DGEBA to 70°C, the acid anhydride curing agent and core-shell particles (dried for 2 h under vacuum at 80°C before use) were added into the epoxy resin under stirring. Then the mixture was placed in a high-energy ultrasonic bath for 15 min to obtain a uniform dispersion. After that, the mixed epoxy system containing a proper content of accelerator was poured into a preheated mold at 115°C and cured for 2 h, and it was postcured at 145°C for 5 h and allowed to cool gradually to room temperature.

The contents of epoxy resin, hardener, and accelerator were 100, 65, and 1 g, respectively. The core-shell particle was employed in ranging from 2 to 15 wt %. The epoxy/core-shell blends were named EPIM0 to EPIM15, according to the core-shell particle content.

### Characterization of the blends

#### Fourier transformed infrared spectroscopy

The FTIR spectra were recorded with a Nicolet AVATAR-IR 360 spectrometer (Nicolet Instrument) by a solid potassium bromide method. Spectra in the optical range of 4000–500  $\text{cm}^{-1}$  were obtained by coadding 20 scans at a resolution of 4  $\text{cm}^{-1}$ .

#### Transmission electron microscopy

The morphology of core-shell particle in the bulk epoxy was observed by a JEOL JEM-100 CX II transmission electron microscope (TEM) with an accelerating voltage of 80 kV. Thin sections of about 70 nm thick from the sample were obtained by ultramicrotomy at an ambient temperature using a Leica Ultracut microtome and a diamond knife. The thin sections were stained with  $\text{OsO}_4$  vapor for 3 h to generate contrast between the phases.

TABLE I  
Chemical Structures of the Reagents and Core-Shell Particles

Materials	Chemical structure
DGEBA	
Curing agent	
Accelerator	
Core-shell particle	

### Scanning electron microscopy

The fracture morphology of epoxy/core-shell particle blends was studied using Hitachi S-2700 scanning electron microscopy (SEM) with an accelerating voltage of 20 kV. The selected specimens were coated with a thin layer of gold prior to microscopy to avoid charge buildup.

### Differential scanning calorimeter

Differential scanning calorimeter (DSC) analysis of the epoxy and its blends was carried out by using a Netzsh DSC 200PC. The calorimeter had previously been calibrated with the indium standard. The temperature error in the DSC is  $\pm 0.2^\circ\text{C}$ . The samples ( $\sim 6$  mg) were heated continuously from room temperature to  $250^\circ\text{C}$  at a heating rate of  $10^\circ\text{C}/\text{min}$ . All measurements were carried out under nitrogen atmosphere.

### Measurements

#### Mechanical test

The specimens for Izod notched impact test were  $4 \pm 0.05$  mm in thickness. These standard specimens were conditioned at the temperature of  $(23 \pm 2)^\circ\text{C}$  and the relative humidity of  $(50 \pm 5)\%$  for 40 h. The Izod notched impact test was assessed according to ASTM D256.

#### Dielectric measurements

The specimens for dielectric measurement were made in the form of circular discs with  $\sim 1$  mm in thickness and 20 mm in diameter. Both sides of the disks were suitably sprayed with gold powder to improve electrical contact. The dielectric measurement was performed on a broadband dielectric spectrometer (Novocontrol Technology Company, Germany) with Alpha-A high performance frequency analyzer. The measurement was carried out in the frequency range from  $10^{-1}$  to  $10^6$  Hz under room temperature. Generally, at least two samples were tested to check reproducibility. All measurements were carried out in the cryostat to avoid possible surrounding effects.

The specimens for dielectric breakdown strength were also 1 mm in thickness. The dielectric breakdown strength of epoxy/core-shell particle blends was measured using a ball-rod electrode arrangement under a continuous ac voltage loading supplied by a 50 kV, 50 Hz transformer. The arrangement and sample were immersed in insulated oil to prevent the surface discharges and flashovers. The test for each sample was performed at room temperature and cryogenic temperature, respectively. For the test at room temperature, the sample was directly placed between

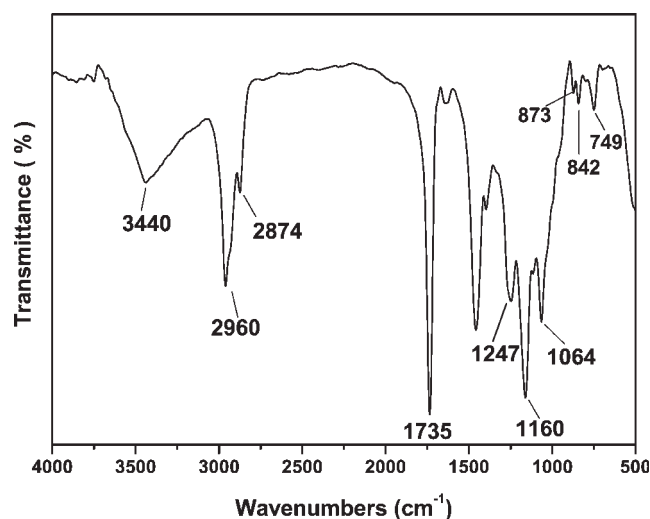


Figure 1 FTIR spectra for the core-shell particles.

the ball and rod electrodes. Then the ultimate breakdown voltage was recorded quickly when the test finished. For the test at cryogenic temperature, firstly the sample was completely immersed into liquid nitrogen for at least 30 min. After that, the cryogenic sample was quickly placed between the ball and rod electrodes. Then the ultimate breakdown voltage was recorded quickly when the test finished. The dielectric breakdown strength of each sample was determined as the average of five tests.

## RESULTS AND DISCUSSION

### Characterization of core-shell particle

#### Surface conditions

The core-shell particle is a type of organic particle with unique structure. Some functional groups may be on the surface. When the particles are added into the epoxy resin, there may be a possibility of some chemical reactions occurring between them. To identify the possibility, therefore, it is necessary to characterize the functional groups on the surface of core-shell particles. Before starting the analysis, the core-shell particles were dried for 2 h under vacuum at  $80^\circ\text{C}$ . In this way, the possible moisture of the core-shell particles absorbed from the environment could be reduced to a minimum. Figure 1 shows the FTIR spectra for the surface of core-shell particles. As expected, in Figure 1, it is seen that the peak at  $3440\text{ cm}^{-1}$  is attributed to the H—O stretch absorption of hydroxyl group, and the peaks at 1247 to  $749\text{ cm}^{-1}$  are attributed to the C—O—C stretch absorption of ester group and epoxy group. Therefore, these groups on the surface of core-shell particles may be reacted with the epoxy matrix during the curing preparation, which in turn would lead to a formation of reactive

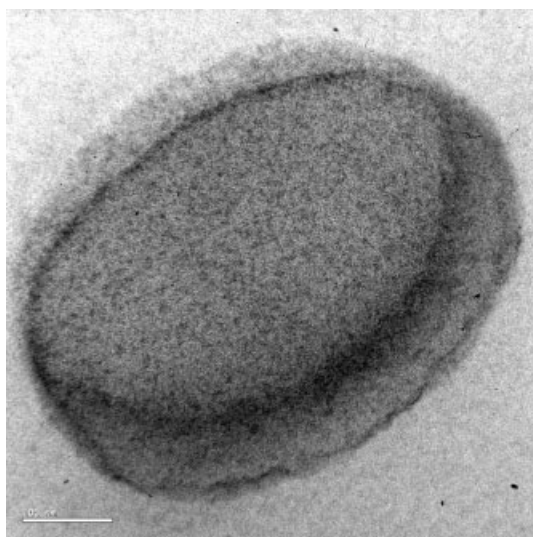


**Figure 2** TEM micrographs of core-shell particle in bulk epoxy.

interfaces in the epoxy blends. As for other groups, peaks presented in the FTIR spectra, although they could not react with the epoxy, may have a well relatively organic compatibility with the epoxy matrix.

#### Morphology in the blend

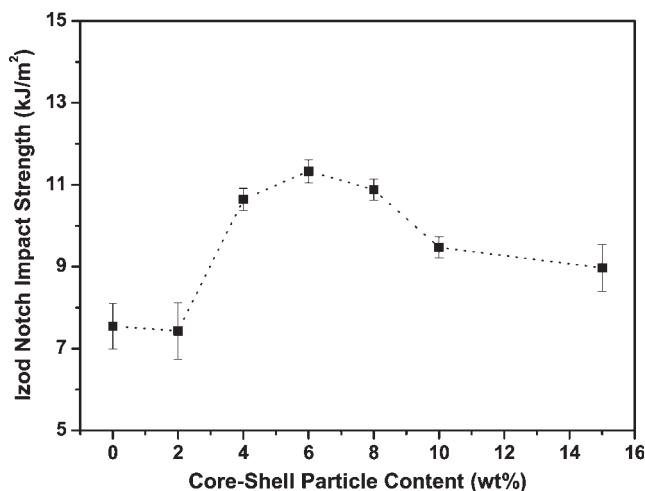
Figure 2 shows the micrograph of core-shell particle in bulk epoxy. In TEM micrograph, the microstructure of the particle with core and shell layers is clearly observed. The particle appears with an average diameter of 400–500 nm and with approximate several nanometers shell layer. In addition, the surrounding of the particle is not easily distinguished from the bulk epoxy, which indicates that there is a compatibility of the core-shell particle with bulk epoxy because of the natural properties of the two organic materials.

#### Mechanical properties of epoxy/core-shell particle blends

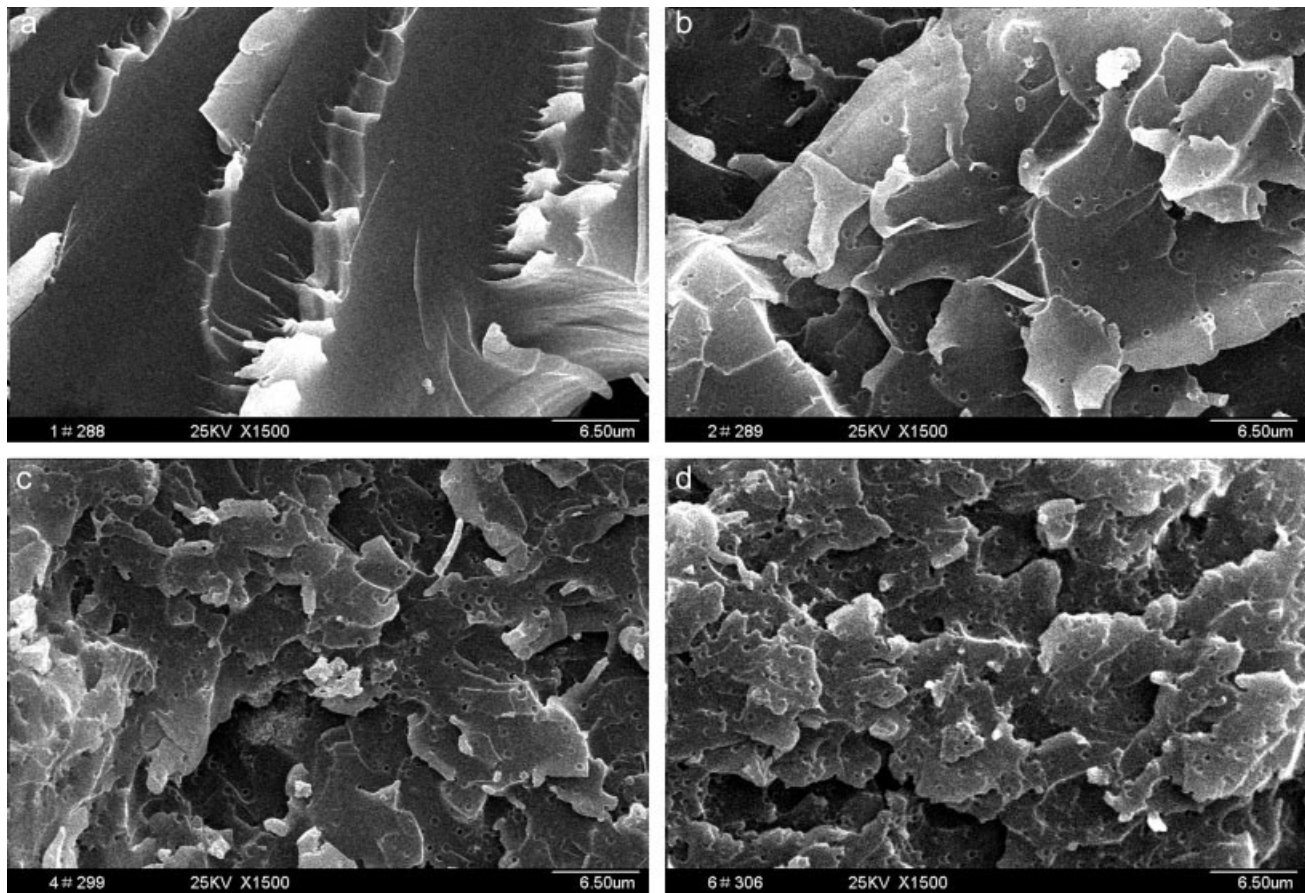
Figure 3 shows the Izod notch impact strength for the epoxy/core-shell particle blends. It can be seen that the impact strength of the epoxy blend firstly gradually increases with increasing core-shell particle content from 0 to 6 wt %, and then decreases slightly with the further increase of the particle content. The impact strength of the epoxy blend reaches the highest value at about 6 wt %, which is ~ 50% higher than that of the neat epoxy. It is clear that the impact strength of the epoxy is greatly improved because of the addition of core-shell particles. For more understanding of the toughness of the epoxy/core-shell particle blends, the fracture surface morphology is observed.

Figure 4 shows SEM micrographs for fracture surfaces of epoxy-based blends with core-shell particles. It

can be seen that the smooth glassy fractured surface with cracks in different planes displays for the neat epoxy resin, which is a typical brittle fracture morphology and leads to poor impact strength. However, as the content of core-shell particles increases, the fracture morphology of epoxy blends shifts and shows the rich characteristics of a toughened fracture surface morphology, as shown in Figure 3(b–d). Since the particle size is large (Fig. 2) enough to allow their deformation energy to be higher than their interfacial bonding to the epoxy matrix, the cavitations will occur during fracture.<sup>12</sup> The generation of the voids arising from the cavitations of core-shell particles is obviously viewed in all samples of epoxy-based blends, which can dissipate the fracture energy when a loading is applied. In addition to that, some stress-whitened zones may be seen from Figure 4(c), which is related with the stress concentration. The local bulk plastic deformation would occur in these zones and absorb impacting energy. Therefore, both the core-shell particle cavitations and the plastic deformation are contributed to the energy absorption in epoxy/core-shell particle blends, which improves the toughness of epoxy-based blends. In Figure 4(d), it is found that more cavitations are introduced with higher core-shell particle content. According to the point of the dissipation of fracture energy, the impact strength of the blend would also be increased. Xiao and Ye reported that there is an average interdistance between core-shell-rubber particles, which plays a very important role on improving fracture toughness of brittle epoxies. They deduced that a critical interdistance between the particles exists, at which the maximum improvement of fracture toughness can be obtained.<sup>13</sup> In our case, it could be considered that the critical interdistance between the core-shell particles becomes smaller at higher particle content, which may weaken



**Figure 3** Impact strength of epoxy and its blends with core-shell particles.



**Figure 4** SEM micrographs for fracture surfaces of modified epoxy with core-shell particles (a) 0 wt %; (b) 2 wt %; (c) 6 wt %; and (d) 10 wt %.

the dissipation of fracture energy. Just as shown in Figure 3, the impact strengths of EPIM6 and EPIM10 are 11.33 and 9.47 kJ/m<sup>2</sup>, respectively. The results of improved toughness of epoxy blends in this study is also in accordance with other works.<sup>13–15</sup> The fine dispersion of core-shell particle in the epoxy blends may also have a contribution to the improved toughness.<sup>16</sup>

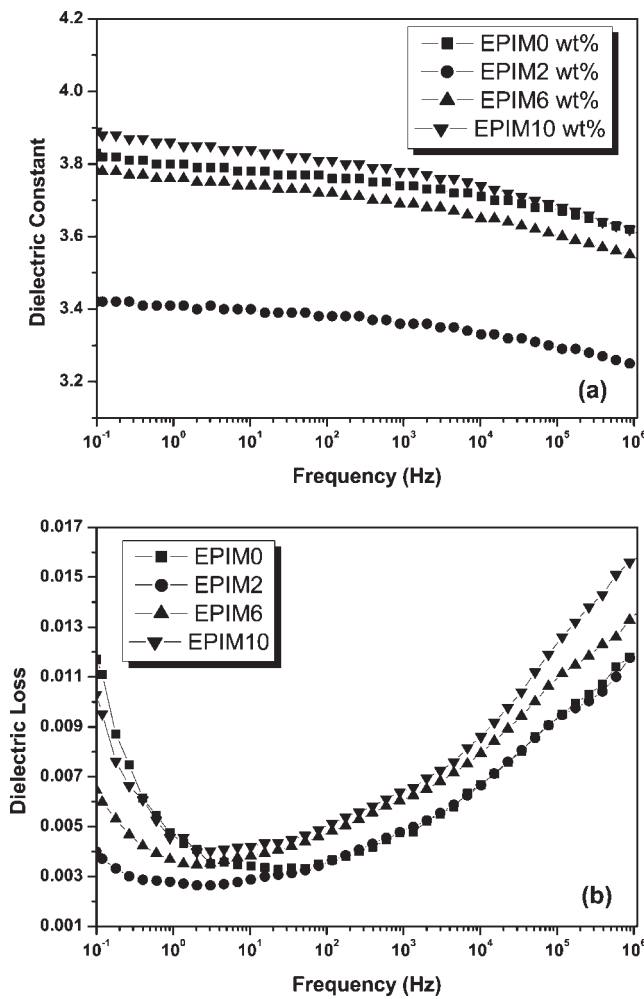
#### Dielectric properties of epoxy/core-shell particle blends

Figure 5 shows the dependence of dielectric constant [Fig. 5(a)] and dielectric loss [Fig. 5(b)] of the neat epoxy and its blends on the frequency range of 10<sup>-1</sup> to 10<sup>6</sup> Hz. It is seen that the dielectric constant of the neat epoxy and its blends at low frequencies (10 Hz) is higher than that at high frequencies (1 MHz), and decreases slowly with the increase of frequency. Over the investigated frequency range, the dielectric constant of the blends with 2 wt % core-shell particles is the lowest among the tested samples. When the core-shell particle content is 6 wt %, it is found that the dielectric constant of the blend is still less than that of the neat epoxy. It is speculated that this may be attributed to interfacial polarization, which will be dis-

cussed in detail later. Therefore, it is concluded that the dielectric constant of the epoxy blends can be reduced with the certain content of the core-shell particles. In Figure 5(b), it is found that the dielectric loss of the neat epoxy and its blends sharply decreases with increasing frequency over a range of 0.1–10 Hz and increases greatly over a frequency range of 10 Hz to 1 MHz. It should also be noted that the dielectric loss of the epoxy blends increases with the content of core-shell particles but still is less than that of the neat epoxy over the frequency range of 0.1–10 Hz. This may be related to complicated interfacial polarization also.

It is well known that a complicated interfacial polarization, which is a kind of dielectric relaxation phenomena, could be initiated when an alternating current field is applied to dielectric materials. Meanwhile, it is considered that the interfacial polarization usually includes the polarization in bulk sample and the sample-electrode interface polarization.

Some researchers have introduced the electric modulus to explain the dielectric relaxation behavior of the polymer.<sup>17–21</sup> Using the electric modulus, the familiar difficulties of electrode nature and contact, space charge injection phenomena and absorbed impurity



**Figure 5** Dependence of (a) dielectric constant and (b) dielectric loss of neat epoxy and its blends on frequency at different contents of core-shell particles at room temperature.

conduction effects, which appear to obscure relaxation in the dielectric constant presentation, can be resolved or even ignored. Therefore, to identify the interfacial polarization in the epoxy blends, the variation of electric modulus will be very helpful. Electric modulus,  $M^*$ , is defined by the following equation:

$$M^* = \frac{1}{\epsilon^*} = \frac{1}{\epsilon' - j\epsilon''} = \frac{\epsilon'}{\epsilon'^2 + \epsilon''^2} + j \frac{\epsilon''}{\epsilon'^2 + \epsilon''^2} = M' + jM'' \quad (1)$$

where  $M'$  is the real and  $M''$  the imaginary electric modulus,  $\epsilon'$  the real and  $\epsilon''$  is the imaginary permittivity.

Figure 6(a,b) show the dependence of the real ( $M'$ ) and imaginary ( $M''$ ) part of electric modulus on the frequency, respectively. In Figure 6(a) it is seen that the  $M'$  of the neat epoxy and its blends at low frequencies (10 Hz) is lower than that at high frequencies (1 MHz), and increases slowly with the increase of fre-

quency. In addition, the  $M'$  of the blends with 2 wt % core-shell particles is the highest among the tested samples. Over the investigated frequency range, therefore, it is found that the variation of  $M'$  of the epoxy blends is inverse to the variation of dielectric constant, as displayed in Figure 5(a). This indicates that the motion of dipoles in the blend with 2 wt % particle content has the biggest contribution to the relaxation in the epoxy blend. It is interesting that the variation of  $M''$  of the epoxy blends is almost the same as the variation of dielectric loss displayed in Figure 6(b), which implies there is no sample-electrode interface polarization during the dielectric measurement.

Therefore, it may be concluded that the sample-electrode interface polarization could be ignored, and here the interfacial polarization in bulk epoxy would be merely discussed. The microdefects are introduced during the preparation process of a polymer, as it is the multiphase polymer material. Consequently, carriers (free electrons and ions, trappings, etc.) would accumulate in the defects, and be polarized under

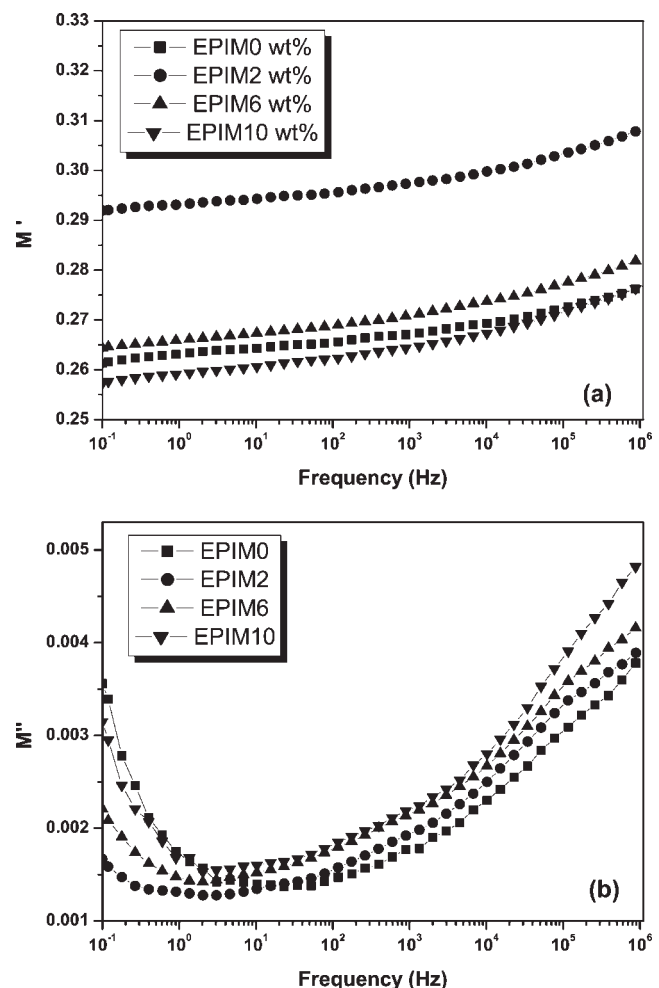


**Figure 6** Dependence of (a) real part and (b) imaginary part of electric modulus of neat epoxy and its blends on frequency at different content of core-shell particles.

applied electrical field. This polarization could affect the internal field distribution in the polymer and lead to a slight increase in both the dielectric constant and the dielectric loss.

In the study of epoxy blends, it is considered that the interfacial polarization in the epoxy/core-shell blends is directly related to the core-shell particles. Figure 1 indicates that interfacial reactions between the core-shell particles and the epoxy resin occurred. Therefore, some reactive interfaces may be formed between the core-shell particles and the bulk epoxy,<sup>16</sup> while other reactive interfaces coming from the core-shell particles by themselves are also introduced. Under an applied electrical field, the motion of dipoles and charge carriers in the epoxy blends may be confined to some extent because of these reactive interfaces, which in turn would weaken the polarization ability of the epoxy resin. In short, this is the most possible explanation for the decrease of dielectric constant and dielectric loss at low frequency range for the epoxy with low core-shell particle content. As far as the increase of dielectric constant and loss of the epoxy blends upon the further addition of core-shell particles is concerned, one may conclude that this is a direct result of the relatively high dielectric constant of the core-shell particles (the  $\epsilon'$  of the core-shell particle is about 5–6, investigated under the same condition).

#### Dielectric breakdown strength of epoxy/core-shell particle blends

The dielectric breakdown strength is an important parameter for the use of polymers as electrical insulation materials. Figure 7 shows the dielectric breakdown strength of the epoxy and its blends as a function of the core-shell particle content at room and cryogenic temperature. It is found that the cryogenic dielectric breakdown strengths of both epoxy and its blends are higher than that at room temperature, while their variations with the core-shell particle content are in similar trends. Furthermore, the dielectric breakdown strength of the blends is lower than that of the epoxy, both at room and cryogenic temperature. Normally, defects in a polymer material would cause the decrease of dielectric breakdown strength because charge carriers may get accumulated. During the preparation of the epoxy blends, defects are carried in the interfacial zones although the interfacial reaction could decrease the formation of defects to some extent. It should be noted that the dielectric breakdown strength of the epoxy blend with 6 wt % of particle content is 27.9 MV/m at room temperature and 29.3 MV/m at cryogenic temperature, which are approximately the same as that of the neat epoxy (28.6 MV/m at room temperature and 30.4 MV/m at cryogenic temperature), as seen in Figure 7. The results

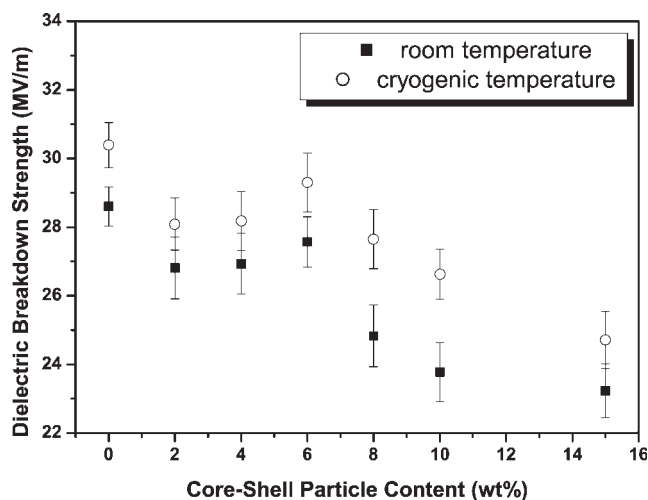


**Figure 7** Effect of core-shell particle content on the dielectric breakdown strength of epoxy/core-shell particle blends at room temperature (■) and cryogenic temperature (○).

could be attributed to the interfacial reaction introduced by the optimum content of core-shell particles. In this case, it is considered that an enough interfacial reaction results in a strong interfacial adhesion in the epoxy blends, which may be the major contribution for the improved dielectric breakdown strength. As a result, the enhanced interfacial adhesion, just as mentioned before, may weaken the mobility of dipoles.

When an external electrical field is applied, the interfacial zones would become the interfacial polarization zones, which could enhance the local field in the bulk epoxy. If the enhanced local field cannot be released in time, the epoxy blends will be broken down in no time under a high continuous ac voltage loading. Studies on increased dielectric breakdown strength by releasing the enhanced local field have been previously reported by other researchers. Nagao et al. reported that the increased dielectric breakdown strength was attributed to an improved electron scattering associated with the increase in polar groups.<sup>22</sup> Yamano and Endoh reported that this resulted from either the trapping effect or the excitation effect of electric dipoles.<sup>23</sup> Ma et al. reported that the increase of dielectric breakdown strength was because of charge scattering or trapping, or excitation effects related to them. They also mentioned that a formed homo charge carrier distribution was beneficial to the improved dielectric breakdown strength.<sup>24</sup> Here, it is considered that the enhanced local fields, originated from the accumulated charge carriers, and may be released through a scattering effect coming from the confined dipoles in the interfacial reaction zones such as reacted molecular groups or nonreacted molecular groups. Therefore, starting from this point, the epoxy blend with optimum content of core-shell particles could be considered as a quasi-homogeneous bulk,

which shows the enhancement of dielectric breakdown strength.

From the above discussion, it can be seen that the enhanced interfacial adhesion due to an optimum content of core-shell particles, corresponding with the reduction of local field, is one reasonable explanation for the improved dielectric breakdown strength of epoxy blends. Furthermore, are there any possible reasons on the basis of molecular motion for the variation of dielectric breakdown strength of the epoxy blends? It has been shown that the variation of free volume also affects the dielectric breakdown strength of polymeric materials. Sabuni and Nelson reported that the dielectric breakdown strength of polystyrene with plasticizer was obviously reduced because of the increase of free volume compared with that of no plasticizer. Moreover, they explained that the dielectric breakdown strength was reduced with the increase of temperature on the view of free volume, and confirmed it by calculation.<sup>25</sup> For a polymer, it is well known that the glass transition temperature,  $T_g$ , is directly related with the free volume. In this study, to deeply understand the mechanism of the variation of dielectric breakdown strength, the glass transition temperature of the neat epoxy and its blends is investigated.

Figure 8 shows an example of DSC curve of epoxy blends, because the DSC curves of these materials have a similar trend without the various glass transition temperatures. The glass transition temperature is obtained from the point of intersection on the curve, shown in Figure 8. Figure 9 shows the variation of  $T_g$  of the neat epoxy and its blends as a function of core-shell particle content. It is clear that the  $T_g$  of the bulk epoxy is obviously changed as the addition of core-shell particles. Especially, the epoxy blend shows the highest  $T_g$  when the core-shell particle content is  $\sim 6$  wt %. Usually toughened polymers

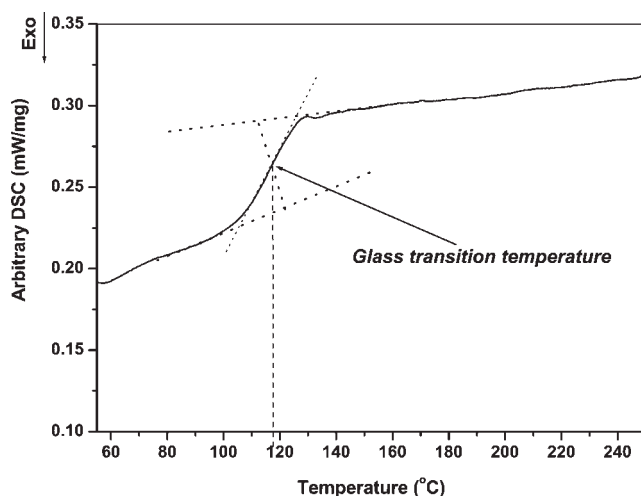


Figure 8 Pattern of glass transition temperature.

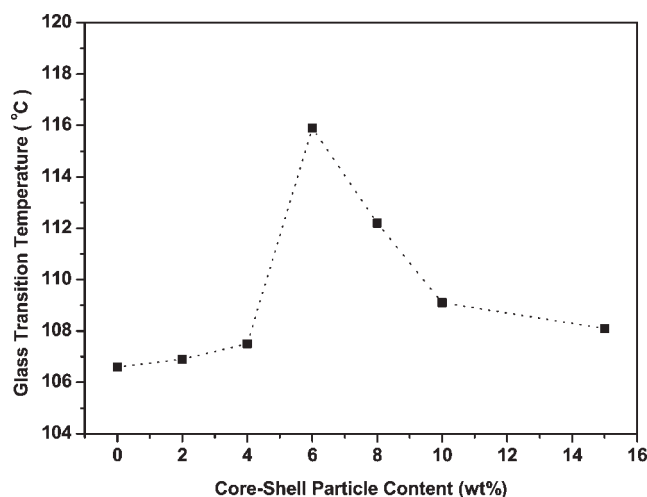


Figure 9 Glass transition temperatures of the neat epoxy and its blends.

show a lower glass transition temperature than that of the based polymers. While for the rigid-rigid toughening mechanism,<sup>26</sup> in the polymer processing, they will be increased simultaneously. In this study, both the toughness and the  $T_g$  are increased for the epoxy blends. Therefore, it may be considered that the improved toughness of our prepared epoxy blends is also due to the toughening mechanism resulting from the unique structure of core-shell particle. The variation of  $T_g$  indicates that the free volume of the bulk epoxy is apparently reduced because of the change of microstructure coming from the interfacial interaction of the neat epoxy and core-shell particles.

It should be noted that the free volume of the epoxy blend reaches the lowest value, whereas the dielectric breakdown strength of the epoxy blend is greatly improved. It is known that the molecular motion of a polymer will be confined because of less space of action if the free volume of the polymer is reduced. Actually, in this study, it may be exactly considered that this is a good condition for the dielectric breakdown strength enhancement of the bulk epoxy. As a result of the reduction of free volume, compared with the neat epoxy, there would not be enough molecular space for the charge carriers to accumulate easily when an external electrical field is applied to the epoxy blends. Therefore, much more polarized charge carriers in the bulk epoxy would be released immediately, which helps the improved dielectric breakdown strength of epoxy blends.

In a short conclusion, as a result of the addition of core-shell particles, it can be considered that the improved dielectric breakdown strength of the epoxy blends is due to two sides: the fine dispersion of an optimum content of core-shell particles and the change of molecular macrostructure.



## CONCLUSIONS

The impact strength and dielectric properties of neat epoxy and epoxy/core-shell particle blends were investigated. It has been shown that the impact strength of epoxy with 6 wt % of core-shell particles increased by ~ 50% compared with the neat epoxy. The improvement in toughness of the epoxy blends was discussed by SEM fracture morphology. The analysis of dielectric behavior showed that the dielectric constant and dielectric loss of the epoxy with a proper content of core-shell particles was lower than that of the neat epoxy at lower frequencies. Meanwhile, the dielectric breakdown strength of the epoxy blends with 6 wt % core-shell particles was similar to the neat epoxy at room and cryogenic temperature. One may conclude that the simultaneously improved toughness and dielectric properties of epoxy/core-shell blends were likely because of fine particle dispersion and enhanced interfacial zones between the core-shell particles and the epoxy resin. Therefore, in this study, all results showed that the epoxy/core-shell particle blends with improved toughness displayed desirable dielectric properties, indicating potential application in insulating of electronic packaging industries.

## References

1. Monizone, L. T.; Gillham, J. K. *J Appl Polym Sci* 1981, 26, 889.
2. Yang, P. C.; Woo, E. P.; Bishop, M. T.; Pickelman, D. M.; Sue, H. *J Polym Mater Sci Eng* 1990, 63, 315.
3. He, S.; Shi, K.; Bai, J.; Zhang, Z.; Li, L.; Du, Z.; Zhang, B. *Polymer* 2001, 42, 9641.
4. Aizpurua, B.; Franco, M.; Corcuera, M. A.; Riccardi, C. C.; Mondragon, I. *J Appl Polym Sci* 2000, 76, 1269.
5. Kang, B. U.; Jho, J. Y. *J Mater Sci Lett* 2001, 20, 375.
6. Qian, J. Y.; Pearson, R. A.; Dimonie, V. L.; Shaffer, O. L.; El-Aasser, M. S. *Polymer* 1997, 38, 21.
7. Ormaetxea, M.; Forcada, J.; Mugika, F.; Valea, A.; Martin, M. D.; Marieta, C.; Goyanes, S.; Mondragon, I. *J Mater Sci* 2001, 36, 854.
8. Fröhlich, J.; Kautz, H.; Thomann, R.; Frey, H.; Mülhaupt, R. *Polymer* 2004, 45, 2155.
9. Day, R. J.; Lovell, P. A.; Wazzan, A. A. *Comp Sci Tech* 2001, 61, 41.
10. Lin, K. F.; Shieh, Y. D. *J Appl Polym Sci* 1998, 69, 2069.
11. Lestriez, B.; Maazouz, A.; Gerard, J. F.; Sautereau, H.; Boiteux, G.; Seytre, G.; Krabuehl, D. E. *Polymer* 1998, 39, 6733.
12. Dompas, D.; Groeninckx, G. *Polymer* 1987, 35, 4743.
13. Xiao, K.; Ye, L. *Polym Eng Sci* 2000, 40, 70.
14. Shen, J. Q.; Zhang, Y. F.; Qiu, J. D.; Kuang, J. Z. *J Mater Sci Lett* 2004, 39, 6383.
15. Lu, F.; Cantwell, W. J.; Kausch, H. H. *J Mater Sci* 1997, 32, 3055.
16. Lin, K. F.; Shieh, Y. D. *J Appl Polym Sci* 1998, 70, 2313.
17. Roling, B. *J Non-Cryst Solids* 1999, 244, 34.
18. Migahed, M. D.; Bakr, N. A.; Abdel-Hamid, M. I.; El-Hanafy, O.; El-Nimr, M. *J Appl Polym Sci* 1996, 59, 655.
19. Bakr, A. A.; North, A. M. *Eur Polym Sci* 1977, 13, 799.
20. Psarras, G. C.; Manolakaki, E.; Tsangaris, G. M. *Compos Part A* 2002, 33, 375.
21. Yu, S. Z.; Hing, P.; Hu, X. *J Appl Phys* 2000, 88, 398.
22. Nagao, M.; Toyoshima, S.; Sawa, G.; Leda, M. *Trans Inst Electr Eng Japan A* 1977, 97, 617.
23. Yamano, Y.; Endoh, H. *IEEE Trans Dielectr Electr Insul* 1998, 5, 270.
24. Ma, D. L.; Hugener, T. A.; Siegel, R. W.; Christerson, A.; Mårtensson, E.; Önnby, C.; Schadler, L. S. *Nanotechnology* 2005, 16, 724.
25. Sabuni, H.; Nelson, J. K. *J Mater Sci* 1979, 14, 2791.
26. Fu, Z. *Strength and Fracture Behaviors of Polymer Materials*; Chemical Industry Press: Beijing, 2005.